Journal of Sound and Vibration (2000) **230**(2), 335–356
doi:10.1006/jsvi.1999.2623, available online at http://www.idealibrary.com on IDEAL®

DIFFERENTIAL QUADRATURE METHOD FOR VIBRATION ANALYSIS OF SHEAR DEFORMABLE ANNULAR SECTOR PLATES

K. M. LIEW AND F.-L. LIU

Centre for Advanced Numerical Engineering Simulations, School of Mechanical and Production Engineering, Nanyang Technological University, Singapore 639798, *Singapore*

(*Received* 10 *September* 1997, *and in final form* 23 *July* 1999)

This paper presents differential quadrature solutions for free vibration analysis of moderately thick annular sector plates based on the Mindlin first-order shear deformation theory. Numerical characteristics of the differential quadrature method are illustrated through solving selected annular sector plates with different boundary conditions, relative thickness ratios, inner-to-outer radius ratios and various sector angles. Parametric studies in terms of the vibration frequency parameters are thoroughly investigated.

© 2000 Academic Press

1. INTRODUCTION

The annular sector plate forms one of the most widely used structural components in engineering applications. The vibration analysis of annular sector plates is, therefore, of paramount importance in practical design. In the past few decades, many researches have been done on the solution of vibration problems of thin annular sector plates by analytical methods [1–5] and numerical methods such as the energy method [6–11], the integral equation method [12], the finite strip method [13] and the spline element method [14, 15], and other methods [16]. In the mean time, the solution of vibration problems of thick annular sector plates has also attracted the attention of many researchers. Kobayashi *et al.* [17] obtained an analytical solution to the vibration of a Mindlin annular sector plate with two radial edges simply supported and two other circular edges free. Huang *et al.* obtained analytical solutions to the sectorial plates having simply supported radial edges and arbitrarily bounded circular edges [18]. Tanaka *et al.* [19] reported solutions to the free vibration of a cantilever annular sector plate with curved radial edges and varying thicknesses. Other researchers obtained numerical solutions for free vibration problems of Reissner or Mindlin annular sector plates by using the finite element method [20, 21], the boundary element method [22], the finite strip method [23, 24] and the Rayleigh–Ritz method [25].

The DQ method was first introduced by Bellman and Casti [26] and Bellman *et al.* [27] and developed further by Quan and Chang [28] and Shu and Richards

 © 2000 Academic Press

[29] into the generalized DQ method through introducing a simple algebraic formula to calculate the weighting coefficients of different derivatives. Many previous studies [30–35] have shown that the DQ method is capable of yielding highly accurate solutions to the initial boundary value problems with much less computational effort. Therefore, it appears that the method has the potential to become an alternative to the conventional numerical methods. However, this powerful method has not been tested to solve the vibration analysis of sector plates.

In this paper, the DQ method is thus applied to the problems of free vibrations of thick Mindlin annular sector plates which are described by three differential equations in a two-dimensional polar co-ordinate system. The accuracy and the convergence characteristics of the DQ method for the free vibration analysis of several thick annular plates of different inner-to-outer radius ratios, relative thickness ratios and boundary conditions are investigated through directly comparing the present results with the existing exact or other numerical solutions. The applicability and the simplicity of the DQ method for the vibration analysis of Mindlin annular sector plates have been demonstrated through solving examples in the parameter studies.

2. METHOD OF DIFFERENTIAL QUADRATURE

The two-dimensional polar co-ordinate system can be treated in a similar way to the two-dimensional Cartesian co-ordinate system in using the differential quadrature rule. Suppose that there are N_R grid points in the R-direction and N_Θ grid points in the Θ direction with $R_1, R_2, \ldots, R_{N_x}$ and $\Theta_1, \Theta_2, \ldots, \Theta_{N_\Theta}$ as the co-ordinates, the nth order partial derivative of $f(R, \Theta)$ with respect to R, the mth order partial derivative of $f(R, \Theta)$ with respect to Θ and the $(n+m)$th order partial derivative of $f(R, \Theta)$ with respect to both R and Θ can be expressed discretely at the point (R_i, Θ_j) as

$$f_R^{(n)}(R_i, \Theta_j) = \sum_{k=1}^{N_R} C_{ik}^{(n)} f(R_k, \Theta_j), \quad n = 1, 2, \ldots, N_R - 1, \tag{1a}$$

$$f_\Theta^{(m)}(R_i, \Theta_j) = \sum_{k=1}^{N_\Theta} \bar{C}_{jk}^{(m)} f(R_i, \Theta_k), \quad m = 1, 2, \ldots, N_\Theta - 1, \tag{1b}$$

$$f_{R\Theta}^{(n+m)}(R_i, \Theta_j) = \sum_{k=1}^{N_R} C_{ik}^{(n)} \sum_{l=1}^{N_\Theta} \bar{C}_{jl}^{(m)} f(R_k, \Theta_l)$$

$$\text{for } i = 1, 2, \ldots, N_R \quad \text{and} \quad j = 1, 2, \ldots, N_\Theta, \tag{1c}$$

where $C_{ij}^{(n)}$ and $\bar{C}_{ij}^{(m)}$ are weighting coefficients associated with nth order partial derivative of $f(R, \Theta)$ with respect to R at the discrete point R_i and mth order derivative with respect to Θ at Θ_j.

According to Quan and Chang [28] and Shu and Richards [29], the weighting coefficients in equations (1a–c) can be determined as follows:

$$C_{ij}^{(1)} = \frac{M^{(1)}(R_i)}{(R_i - R_j)M^{(1)}(R_j)}, \quad i, j = 1, 2, \ldots, N_R, \text{ but } j \neq i, \tag{2}$$

where

$$M^{(1)}(R_i) = \prod_{j=1,\, j \neq i}^{N_R} (R_i - R_j) \tag{3}$$

and

$$C_{ij}^{(n)} = n\left(C_{ii}^{(n-1)} C_{ij}^{(1)} - \frac{C_{ij}^{(n-1)}}{R_i - R_j}\right) \tag{4}$$

for $i, j = 1, 2, \ldots, N_R$, but $j \neq i$; and $n = 2, 3, \ldots, N_R - 1$,

$$C_{il}^{(n)} = -\sum_{j=1,\, j \neq i}^{N_R} C_{ij}^{(n)}, \quad i = 1, 2, \ldots, N_R, \quad \text{and} \quad n = 1, 2, \ldots, N_R - 1. \tag{5}$$

$\bar{C}_{ij}^{(n)}$ can be determined using equations (1)–(5) simply by replacing all R with Θ.

3. MODELLING OF PROBLEMS BY DQ METHOD

3.1. GOVERNING EQUATIONS

The problem concerned here is the transverse free vibration of a thick isotropic annular sector plate with uniform thickness h, sector angle α, inner radius b and outer radius a as shown in Figure 1. According to Mindlin's plate theory, the equilibrium equations in terms of moment and shear resultants in polar co-ordinates are [36]

$$\frac{\partial M_r}{\partial r} + \frac{1}{r}\frac{\partial M_{r\theta}}{\partial \theta} + \frac{1}{r}(M_r - M_\theta) - Q_r = \frac{\rho h^3}{12}\frac{\partial^2 \psi_r}{\partial t^2}, \tag{6a}$$

$$\frac{\partial M_{r\theta}}{\partial r} + \frac{1}{r}\frac{\partial M_\theta}{\partial \theta} + \frac{2}{r}M_{r\theta} - Q_\theta = \frac{\rho h^3}{12}\frac{\partial^2 \psi_\theta}{\partial t^2}, \tag{6b}$$

$$\frac{\partial Q_r}{\partial r} + \frac{1}{r}\frac{\partial Q_\theta}{\partial \theta} + \frac{1}{r}Q_r = \rho h\frac{\partial^2 w}{\partial t^2}, \tag{6c}$$

where ρ is the density of the plate. The moment resultants M_r, M_θ, and $M_{r\theta}$ and the force resultants Q_r and Q_θ are expressed by the transverse deflection w and the

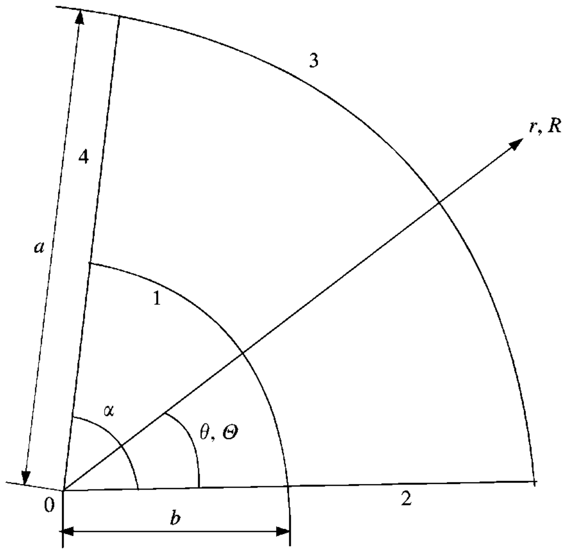

Figure 1. Geometry and co-ordinate system of annular sector plate.

bending rotations ψ_r in the radial plane and ψ_θ in the circumferential plane as follows:

$$M_r = D\left(\frac{\partial \psi_r}{\partial r} + \nu \frac{1}{r}\left(\psi_r + \frac{\partial \psi_\theta}{\partial \theta}\right)\right), \tag{7a}$$

$$M_\theta = D\left(\frac{1}{r}\left(\psi_r + \frac{\partial \psi_\theta}{\partial \theta}\right) + \nu \frac{\partial \psi_r}{\partial r}\right), \tag{7b}$$

$$M_{r\theta} = \frac{1-\nu}{2} D\left(\frac{1}{r}\left(\frac{\partial \psi_r}{\partial \theta} - \psi_\theta\right) + \frac{\partial \psi_\theta}{\partial r}\right) \tag{7c}$$

and

$$Q_r = \kappa G h\left(\psi_r + \frac{\partial w}{\partial r}\right), \tag{8a}$$

$$Q_\theta = \kappa G h\left(\psi_\theta + \frac{1}{r}\frac{\partial w}{\partial \theta}\right), \tag{8b}$$

where

$$D = \frac{Eh^3}{12(1-\nu^2)} \tag{9}$$

and E, G and v are Young's modulus, shear modulus and the Poisson ratio of the plate respectively, and κ is the shear correction factor.

Using the following dimensionless parameters,

$$R = r/a,\ \Theta = \theta/\alpha,\ W = w/a,\ \Psi_R = \psi_r,\ \Psi_\Theta = \psi_\theta,\ \delta = h/a, \tag{10a}$$

$$T = t/t_0, \quad t_0 = \sqrt{\frac{\rho a^2(1-v^2)}{E}}, \tag{10b}$$

and substituting equations (7) and (8) into equation (6), one can normalize the governing equations as follows:

$$R^2\frac{\partial^2\Psi_R}{\partial R^2} + R\frac{\partial\Psi_R}{\partial R} - (1+\xi R^2)\Psi_R + \frac{(1-v)}{2\alpha^2}\frac{\partial^2\Psi_R}{\partial\Theta^2} + \frac{(1+v)}{2\alpha}R\frac{\partial^2\Psi_\Theta}{\partial R\partial\Theta}$$

$$-\frac{(3-v)}{2\alpha}\frac{\partial\Psi_\theta}{\partial\Theta} - \xi R^2\frac{\partial W}{\partial R} = R^2\frac{\partial^2\Psi_R}{\partial T^2}, \tag{11a}$$

$$\frac{(1+v)}{2}R\frac{\partial^2\Psi_R}{\partial R\partial\Theta} + \frac{(3-v)}{2\alpha}\frac{\partial\Psi_R}{\partial\Theta} + \frac{1}{\alpha^2}\frac{\partial^2\Psi_\Theta}{\partial\Theta^2} + \frac{(1-v)}{2}R^2\frac{\partial^2\Psi_\Theta}{\partial R^2}$$

$$+\frac{(1-v)}{2}R\frac{\partial\Psi_\Theta}{\partial R} - \left[\frac{(1-v)}{2} + \xi R^2\right]\Psi_\Theta - \frac{\xi}{\alpha}R\frac{\partial W}{\partial\Theta} = R^2\frac{\partial^2\Psi_\Theta}{\partial T^2}, \tag{11b}$$

$$\left(R^2\frac{\partial^2 W}{\partial R^2} + R\frac{\partial W}{\partial R} + \frac{1}{\alpha^2}\frac{\partial^2 W}{\partial\Theta^2}\right) + \left(R^2\frac{\partial\Psi_R}{\partial R} + R\Psi_R\right)$$

$$+\frac{R}{\alpha}\frac{\partial\Psi_\Theta}{\partial\Theta} = \frac{2R^2}{\kappa(1-v)}\frac{\partial^2 W}{\partial T^2}, \tag{11c}$$

where

$$\xi = \frac{6\kappa(1-v)}{\delta^2} \tag{12}$$

and the stress-displacement relationships are given by

$$\overline{M}_R = \frac{\partial\Psi_R}{\partial R} + v\frac{1}{R}\left(\Psi_R + \frac{1}{\alpha}\frac{\partial\Psi_\Theta}{\partial\Theta}\right), \tag{13a}$$

$$\overline{M}_\Theta = \frac{1}{R}\left(\Psi_R + \frac{1}{\alpha}\frac{\partial\Psi_\Theta}{\partial\Theta}\right) + v\frac{\partial\Psi_R}{\partial R}, \tag{13b}$$

$$\overline{M}_{R\Theta} = \frac{1-v}{2}\left[\frac{1}{R}\left(\frac{1}{\alpha}\frac{\partial\Psi_R}{\partial\Theta} - \Psi_\Theta\right) + \frac{\partial\Psi_\Theta}{\partial R}\right], \tag{13c}$$

where $\overline{M}_R = M_r/(D/a)$, $\overline{M}_\Theta = M_\theta/(D/a)$ and $\overline{M}_{R\Theta} = M_{r\theta}/(D/a)$.

For free vibration, the solutions of motion in time can be assumed as

$$W(R,\Theta,T)=W_j(R,\Theta)\mathrm{e}^{\mathrm{i}\Omega_j T},\quad \Psi_R(R,\Theta,T)=\Psi_{Rj}(R,\Theta)\mathrm{e}^{\mathrm{i}\Omega_j T},$$

$$\Psi_\Theta(R,\Theta,T)=\Psi_{\Theta j}(R,\Theta)\mathrm{e}^{\mathrm{i}\Omega_j T}, \tag{14a, b, c}$$

where Ω_j is the eigenvalue of the jth mode of vibration.

Substitution of equation (14) into equation (11) leads to

$$R^2\frac{\partial^2\Psi_R}{\partial R^2}+R\frac{\partial\Psi_R}{\partial R}-(1+\xi R^2)\Psi_R+\frac{(1-\nu)}{2\alpha^2}\frac{\partial^2\Psi_R}{\partial\Theta^2}+\frac{(1+\nu)}{2\alpha}R\frac{\partial^2\Psi_\Theta}{\partial R\partial\Theta}$$

$$-\frac{(3-\nu)}{2\alpha}\frac{\partial\Psi_\Theta}{\partial\Theta}-\xi R^2\frac{\partial W}{\partial R}=-R^2\Omega^2\Psi_R, \tag{15a}$$

$$\frac{(1+\nu)}{2\alpha}R\frac{\partial^2\Psi_R}{\partial R\partial\Theta}+\frac{(3-\nu)}{2\alpha}\frac{\partial\Psi_R}{\partial\Theta}+\frac{1}{\alpha^2}\frac{\partial^2\Psi_\Theta}{\partial\Theta^2}+\frac{(1-\nu)}{2}R^2\frac{\partial^2\Psi_\Theta}{\partial R^2}$$

$$+\frac{(1-\nu)}{2}R\frac{\partial\Psi_\Theta}{\partial R}-\left[\frac{(1-\nu)}{2}+\xi R^2\right]\Psi_\Theta-\frac{\xi}{\alpha}R\frac{\partial W}{\partial\Theta}=-R^2\Omega^2\Psi_\Theta, \tag{15b}$$

$$\left(R^2\frac{\partial^2 W}{\partial R^2}+R\frac{\partial W}{\partial R}+\frac{1}{\alpha^2}\frac{\partial^2 W}{\partial\Theta^2}\right)+\left(R^2\frac{\partial\Psi_R}{\partial R}+R\Psi_R\right)$$

$$+\frac{R}{\alpha}\frac{\partial\Psi_\Theta}{\partial\Theta}=-\frac{2R^2}{\kappa(1-\nu)}\Omega^2 W \tag{15c}$$

in which and also in the following, W, Ψ_R, Ψ_Θ and Ω should have been taken as $W_j(R,\Theta)$, $\Psi_{Rj}(R,\Theta)$, $\Psi_{\Theta j}(R,\Theta)$ and Ω_j respectively for the jth mode of vibration, but the suffix j is omitted for the sake of convenience.

According to the differential quadrature procedure, the normalized governing equations (15) will be transformed into the following discrete forms:

$$\left[\sum_{k=1}^{N_R}(C_{ik}^{(2)}R_i^2+C_{ik}^{(1)}R_i)\Psi_R(k,j)\right]-(1+\xi R_i^2)\Psi_R(i,j)$$

$$+\frac{1-\nu}{2}\beta^2\left[\sum_{m=1}^{N_\Theta}\bar{C}_{jm}^{(2)}\Psi_R(i,m)\right]+\frac{1+\nu}{2}\beta R_i\left[\sum_{k=1}^{N_R}C_{ik}^{(1)}\sum_{m=1}^{N_\Theta}\bar{C}_{jm}^{(1)}\Psi_\Theta(k,m)\right]$$

$$-\frac{(3-\nu)}{2}\beta\left[\sum_{m=1}^{N_\Theta}\bar{C}_{jm}\Psi_\Theta(i,m)\right]-\xi R_i^2\left[\sum_{k=1}^{N_R}C_{ik}^{(1)}W(k,j)\right]=-\Omega^2R_i^2\Psi_R(i,j), \tag{16a}$$

$$\frac{1+v}{2}\beta R_i\left[\sum_{k=1}^{N_R} C_{ik}^{(1)}\sum_{m=1}^{N_\Theta}\bar{C}_{jm}^{(1)}\Psi_R(k,m)\right]+\frac{3-v}{2}\beta\left[\sum_{m=1}^{N_\Theta}\bar{C}_{jm}^{(1)}\Psi_R(i,m)\right]$$

$$+\beta^2\left[\sum_{m=1}^{N_\Theta}\bar{C}_{jm}^{(2)}\Psi_\Theta(i,m)\right]+\frac{1-v}{2}\left[\sum_{k=1}^{N_R}(C_{ik}^{(2)}R_i^2+C_{ik}^{(1)}R_i)\Psi_\Theta(k,j)\right]$$

$$-\left(\frac{1-v}{2}+\xi R_i^2\right)\Psi_\Theta(i,j)-\xi\beta R_i\left[\sum_{m=1}^{N_\Theta}\bar{C}_{jm}^{(1)}W(i,m)\right]=-\Omega^2R_i^2\Psi_\Theta(i,j), \tag{16b}$$

$$\left[\sum_{k=1}^{N_R}(C_{ik}^{(2)}R_i^2+C_{ik}^{(1)}R_i)W(k,j)\right]+\beta^2\left[\sum_{m=1}^{N_\Theta}\bar{C}_{jm}^{(2)}W(i,m)\right]+R_i^2\left[\sum_{k=1}^{N_R}C_{ik}^{(1)}\Psi_R(k,j)\right]$$

$$+R_i\Psi_R(i,j)+\beta R_i\left[\sum_{m=1}^{N_\Theta}\bar{C}_{jm}^{(1)}\Psi_\Theta(i,m)\right]=-\frac{2}{\kappa(1-v)}\Omega^2R_i^2W(i,j), \tag{16c}$$

where $i=2,\ldots,N_R-1$ and $j=2,\ldots,N_\Theta-1$. $C_{rs}^{(n)}$ and $\bar{C}_{rs}^{(n)}$ are the weighting coefficients for the nth order partial derivatives of W, Ψ_R and Ψ_Θ with respect to R and Θ respectively.

It should be noticed that the domain $[b/a, 1]$ of dimensionless variable R is not the often used [0, 1] or [−1, 1]. Therefore, the DQ weighting coefficients, $C_{rs}^{(n)}$ and $\bar{C}_{rs}^{(n)}$, are different from the standard ones corresponding to the [0, 1] or [−1, 1] domain.

3.2. BOUNDARY CONDITIONS

The boundary conditions considered herein are divided into four kinds. Taking the radial edge with θ = constant, for example, we have

Simply supported edge (S): $w=M_\theta=\psi_r=0$, (17)

(S′): $w=M_\theta=M_{r\theta}=0$, (18)

Clamped edge (C): $w=\psi_r=\psi_\theta=0$, (19)

Free edge (F): $Q_\theta=M_\theta=M_{r\theta}=0$. (20)

Substituting equations (7) and (8) into equations (17)–(20) and normalizing them lead to

Simply supported edge (S):

$$W=0,\quad vR\frac{\partial\Psi_R}{\partial R}+\Psi_R+\frac{1}{\alpha}\frac{\partial\Psi_\Theta}{\partial\Theta}=0,\quad \Psi_R=0. \tag{21}$$

Simply supported edge (S′):

$$W = 0, \quad vR\frac{\partial \Psi_R}{\partial R} + \Psi_R + \frac{1}{\alpha}\frac{\partial \Psi_\Theta}{\partial \Theta} = 0, \quad \frac{1}{\alpha}\frac{\partial \Psi_R}{\partial \Theta} - \Psi_\Theta + R\frac{\partial \Psi_\Theta}{\partial R} = 0. \tag{22}$$

Clamped edge (C):

$$W = 0, \quad \Psi_R = 0, \quad \Psi_\Theta = 0 \tag{23}$$

Free edge (F):

$$\frac{1}{\alpha}\frac{\partial W}{\partial \Theta} + R\Psi_\Theta = 0, \quad vR\frac{\partial \Psi_R}{\partial R} + \Psi_R + \frac{1}{\alpha}\frac{\partial \Psi_\Theta}{\partial \Theta} = 0, \quad \frac{1}{\alpha}\frac{\partial \Psi_R}{\partial \Theta} - \Psi_\Theta + R\frac{\partial \Psi_\Theta}{\partial R} = 0. \tag{24}$$

Using the DQ procedure, the normalized boundary conditions presented by equations (21)–(24) for an edge of $\Theta =$ constant, can then be described in the following discrete forms. For an example, at the edge $\Theta = 0$:

(S) $$W_{i1} = 0, \tag{25a}$$

$$vR_i \sum_{k=1}^{N_R} C_{k1}^{(1)} \Psi_R(k, 1) + \Psi_R + \frac{1}{\alpha} \sum_{m=1}^{N_\Theta} \bar{C}_{1m}^{(1)} \Psi_\Theta(i, m) = 0, \tag{25b}$$

$$\Psi_R(i, 1) = 0. \tag{25c}$$

(S′) $$W_{1j} = 0, \tag{26a}$$

$$vR_i \sum_{k=1}^{N_R} C_{k1}^{(1)} \Psi_R(k, 1) + \Psi_R + \frac{1}{\alpha} \sum_{m=1}^{N_\Theta} \bar{C}_{1m}^{(1)} \Psi_\Theta(i, m) = 0, \tag{26b}$$

$$\frac{1}{\alpha} \sum_{m=1}^{N_\Theta} \bar{C}_{1m}^{(1)} \Psi_R(i, m) - \Psi_\Theta(i, 1) + R_i \sum_{k=1}^{N_R} C_{ik}^{(1)} \Psi_\Theta(k, 1) = 0, \tag{26c}$$

(C) $$W_{i1} = 0, \tag{27a}$$

$$\Psi_R(i, 1) = 0, \tag{27b}$$

$$\Psi_\Theta(i, 1) = 0, \tag{27c}$$

(F) $$\frac{1}{\alpha} \sum_{k=1}^{N_\Theta} \bar{C}_{1k}^{(1)} W(i, m) + R_i \Psi_\Theta(i, 1) = 0, \tag{28a}$$

$$vR_i \sum_{k=1}^{N_R} C_{k1}^{(1)} \Psi_R(k, 1) + \Psi_R + \frac{1}{\alpha} \sum_{m=1}^{N_\Theta} \bar{C}_{1m}^{(1)} \Psi_\Theta(i, m) = 0, \tag{28b}$$

$$\frac{1}{\alpha}\sum_{m=1}^{N_\Theta}\bar{C}_{1m}^{(1)}\Psi_R(i,m)-\Psi_\Theta(i,1)+R_i\sum_{k=1}^{N_R}C_{ik}^{(1)}\Psi_\Theta(k,1)=0,$$

$$i=1,2,\ldots,N_R \text{ for equations (25a)–(28c).} \tag{28c}$$

For the edge of $\Theta=1$, the discrete boundary conditions can be simply obtained by substituting all the subscripts of 1 into equations (25)–(28) with N_Θ. The boundary conditions for the circular edge with $R=$ constant can also be written in the same manner.

4. NUMERICAL RESULTS AND DISCUSSION

Based on the formulas presented in the previous section, a programme has been built up to solve the eigenvalues of the plate. For all the calculations here, the Poisson ratio and the shear correction factor κ have been taken as $\nu=0{\cdot}3$ and $\pi^2/12$. The grid points employed in computation are designated by

$$R_i=\left\{b+\frac{1}{2}\left[1-\cos\left(\frac{(i-1)\pi}{N_R-1}\right)\right](a-b)\right\}\Big/a,\quad i=1,2,\ldots,N_R, \tag{29a}$$

$$\Theta_j=\frac{1}{2}\left[1-\cos\left(\frac{(j-1)\pi}{N_\Theta-1}\right)\right],\quad j=1,2,\ldots,N_\Theta. \tag{29b}$$

The moderately thick isotropic plates with six different boundary conditions of SSSS, CCCC, CSCS, CFCF, FCSC and SCFC have been considered here. The symbol FCSC, for instance, represents the free, clamped, simply supported and clamped boundary conditions of edges 1, 2, 3 and 4 on the plate shown in Figure 1 respectively. The eigenvalues are expressed in terms of non-dimensional frequency parameter λ^2 which is defined as follows:

$$\lambda^2=\omega a^2\sqrt{\frac{\rho h}{D}}\quad\text{and}\quad\omega=\Omega\sqrt{\frac{E}{\rho a^2(1-\nu^2)}}. \tag{30}$$

4.1. CONVERGENCE AND ACCURACY STUDIES

The convergence studies of the DQ method for free vibration of annular sector Mindlin plates should be carried out first to reveal the convergence characteristics of this numerical method for the problem concerned and also to ensure the accuracy of the present results. In the mean time, the effects of boundary conditions, relative thickness, inner-to-outer cut-out ratio and sector angle on the convergence properties should also be investigated so that the number of grid points required for an effective solution of the problem can be determined.

Figures 2–4 show the convergence patterns of an annular sector plate with SSSS, CCCC and CSCS boundary conditions respectively. The normalized frequency

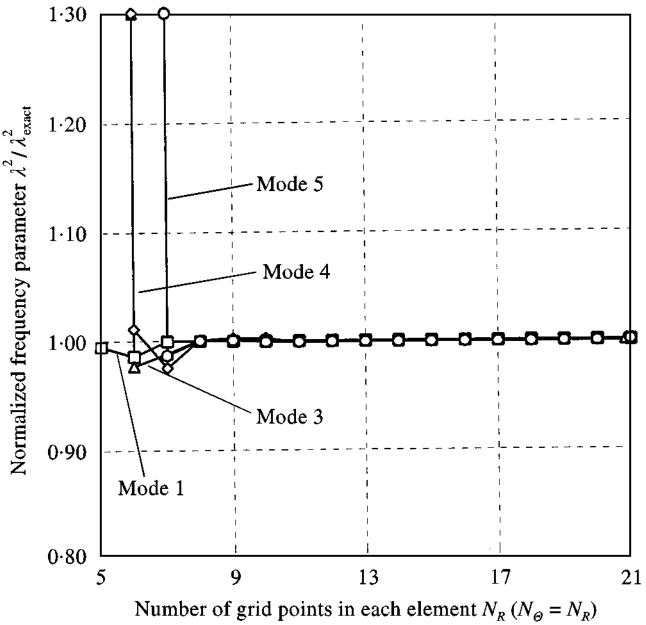

Figure 2. Convergence pattern of normalized frequency parameter $\lambda^2/\lambda^2_{\text{exact}}$ of modes 1, 3, 4 and 5 for a simply supported annular sector plate.

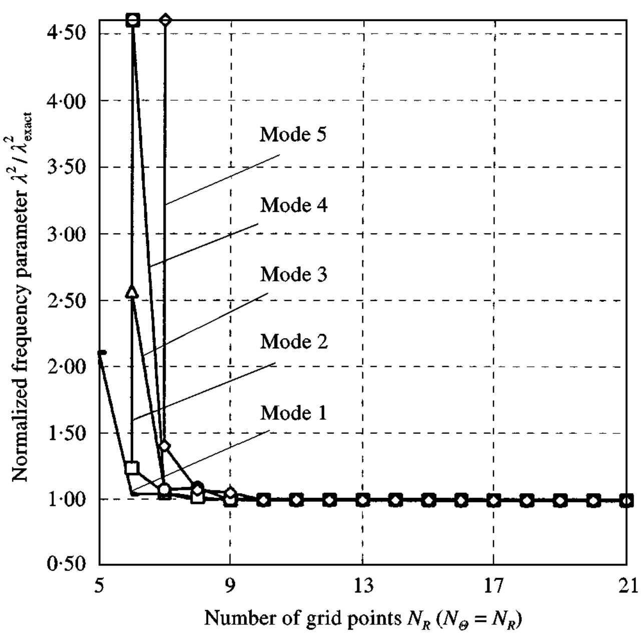

Figure 3. Convergence pattern of normalized frequency parameter $\lambda^2/\lambda^2_{\text{exact}}$ of first five modes for a fully clamped annular sector plate.

parameters $\lambda^2/\lambda^2_{\text{exact}}$ of the first five mode sequences are presented in these figures, and the values of λ^2_{exact} are the exact solutions taken from Ramakrishnan and Kunikkasseril [2]. The convergence pattern of CFCF annular sector plate is shown

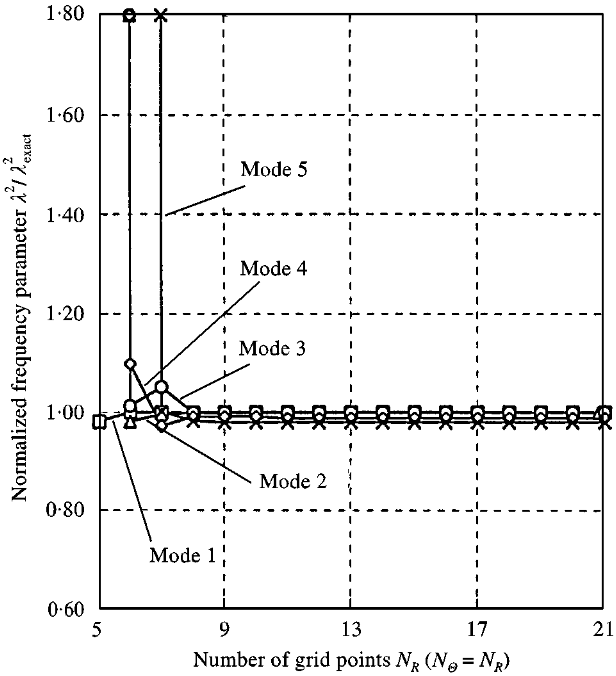

Figure 4. Convergence pattern of normalized frequency parameter $\lambda^2/\lambda^2_{\text{exact}}$ of first five modes for an annular sector plate with CSCS boundary conditions.

in Figure 5 and the parameter λ_c^2 stands for the completely converged DQ results (with five significant digits). In Figures 2, 4 and 5, the sector angle α and the inner-to-outer cut-out ratio b/a are taken to be 45° and 0·5 respectively, whereas in Figure 3, the value of α and b/a are 90° and 0·00001 respectively so that the direct comparison can be made between the present DQ results and the existing exact solutions [2]. For all the four cases, the relative thickness h/a is taken to be 0·005. From these figures, it is found that (1) for all the four kinds of boundary conditions considered here, the DQ results of the annular sector plates converge to the exact solutions (Figures 2–4) or the corresponding converged values with the increase of the grid points (Figure 5); (2) among the DQ results of these four cases, only the fully clamped plate (CCCC) demonstrates the monotonic convergence pattern, while all other cases (SSSS, CSCS and CFCF) show the fluctuating characteristics in the convergence patterns; (3) for different mode sequences, the convergent speeds are different. Normally, the higher the mode sequence, the slower the convergent speed; (4) for all the mode sequences, the boundary condition plays the most important part in the convergent speed of DQ solutions for the free vibrations of annular sector plates. For example, for the fully clamped, simply supported boundary condition and their combinations, all the frequency parameters completely converge to their corresponding converged values when the number of the grid points for each co-ordinate variable is equal to or greater than 11, whereas for the CFCF plate, even when the number of grid points for each co-ordinate is equal to 25, the results are still fluctuating slightly.

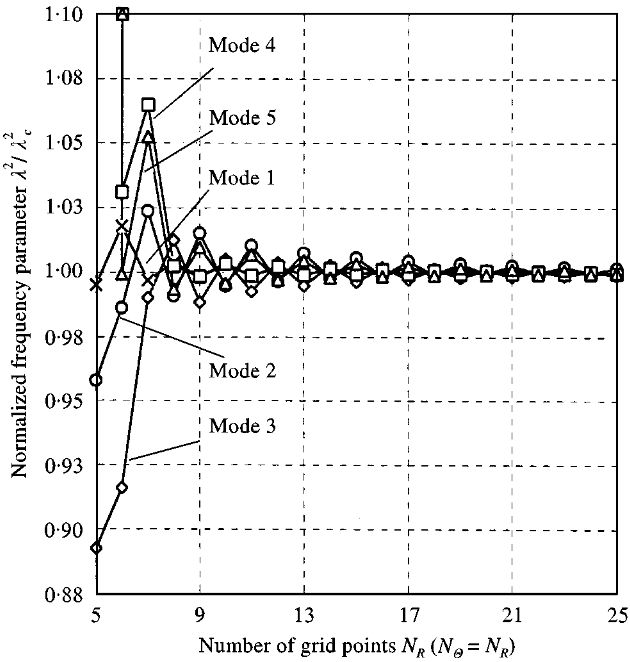

Figure 5. Convergence pattern of normalized frequency parameter $\lambda^2/\lambda^2_{exact}$ of first five modes for an annular sector plate with CFCF boundary conditions.

In order to further reveal the effects of other parameters such as relative thickness h/a, sector angle α, and the inner-to-outer cut-out ratio b/a, the most difficult convergent case CFCF among the six cases concerned in this paper is selected. Figure 6 shows the effects of plate thickness h/a on the convergence of the frequency parameter λ^2 of the first and the fourth modes. It is observed that the relative thickness h/a has the significant effects on the convergent speed of the DQ solutions. The thicker a plate is ($h/a = 0{\cdot}005$–$0{\cdot}2$), the faster the convergent speed for both the fundamental frequency and the higher mode of frequencies. In other words, increasing the relative thickness h/a from 0·005 to 0·2 can greatly improve the convergence ratio of the DQ results with the refinement of the grid. The effects of the sector angle on the convergence of frequency parameter λ^2 of the first and the third modes for the annular sector plate are illustrated in Figure 7. It is very clear to see that for the fundamental frequency (Figure 7(a)), with the increase of the sector angle (in the range of 30–120°), the convergent rate increases, but for the higher mode such as the third mode (Figure 7(b)), this conclusion is only true for the grid points of each co-ordinate variable between 5 and 12; if the grid points along each co-ordinate direction are over 13, the value of the sector angle will almost bear no effects on the convergent rate. Figure 8 shows the effects of the inner-to-outer cut-out ratio on the convergence of frequency parameter λ^2 of the first and the third modes of the annular sector plate. It is also found that the inner-to-outer cut-out ratio b/a can only have the effect on the convergence patterns when the grid points for each co-ordinate variable are smaller than 14; when the grid points are larger

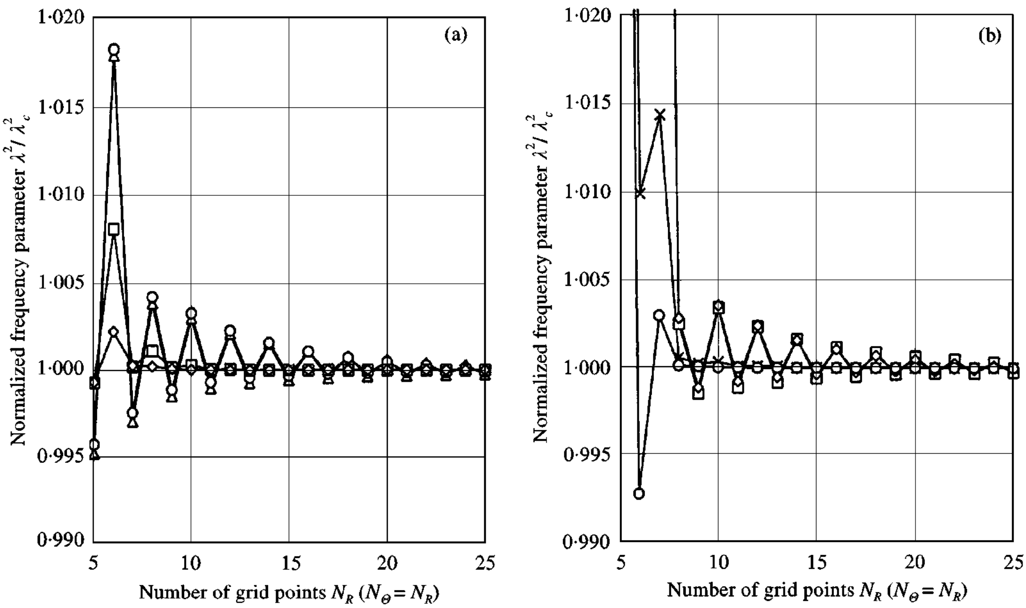

Figure 6. Effects of plate thickness h/a on convergence of normalized frequency parameter λ^2/λ_c^2 of annular sector plate with CFCF boundary conditions: (a) mode 1 —△—, $h/a = 0{\cdot}005$; —○—, $h/a = 0{\cdot}01$; —□—, $h/a = 0{\cdot}1$; —◇—, $h/a = 0{\cdot}2$; (b) mode 4. —□—, $h/a = 0{\cdot}005$; —◇—, $h/a = 0{\cdot}01$; —×—, $h/a = 0{\cdot}1$; —○—, $h/a = 0{\cdot}2$.

than 14, the convergent rates for both of the first and the fifth modes of the frequency parameter λ^2 are completely dominated by the number of the grid points.

To examine the accuracy of the converged DQ results, comparisons with the earlier results obtained by using other methods such as the analytical method [2], the Mindlin finite-strip method [15] and the Rayleigh–Ritz method [25] are made for four boundary conditions (SSSS, CCCC, CSCS and CFCF) in Table 1. It is observed that close agreement has been obtained for all the cases presented in the table.

4.2. PARAMETRIC STUDIES

The first six natural frequencies of the annular sector plates with six boundary conditions, different relative thicknesses, different sector angles and inner-to-outer radius ratios are computed by using the DQ method and presented in Tables 2–7. The values of sector angle, relative thickness and inner-to-outer radius ratio are taken as $\alpha = 30$, 60, and 120°, $h/a = 0{\cdot}01$, $0{\cdot}1$ and $0{\cdot}2$ and $b/a = 0{\cdot}1$, $0{\cdot}25$ and $0{\cdot}5$ respectively in the calculation. All the results shown in these tables are completely converged ones with five significant digits for the thick plates and four significant digits for the thin plates. Based on the results in all these tables, the following conclusion remarks can be made:

(1) As the sector angle increases, for the annular sector plate with SSSS, CCCC, CSCS, FCSC and SCFC boundary conditions, he first six frequency parameters decrease significantly for any given relative thickness h/a and

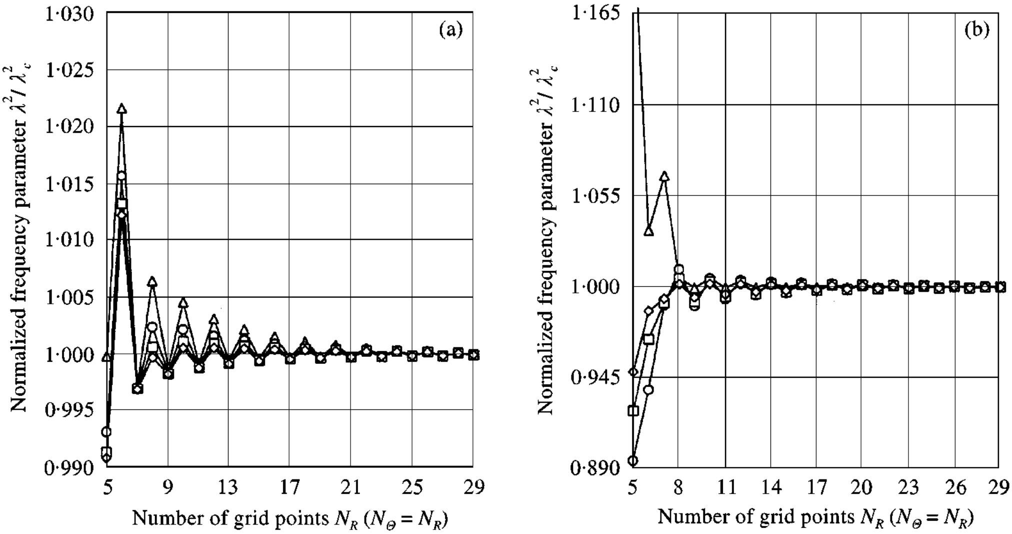

Figure 7. Effects of sector angle α on convergence of normalized frequency parameter λ^2/λ_c^2 of annular sector plate with CFCF boundary conditions: (a) mode 1; (b) mode 3. —△—, $\alpha = 30$; —○—, $\alpha = 60$; —□—, $\alpha = 90$; —◇—, $\alpha = 120$.

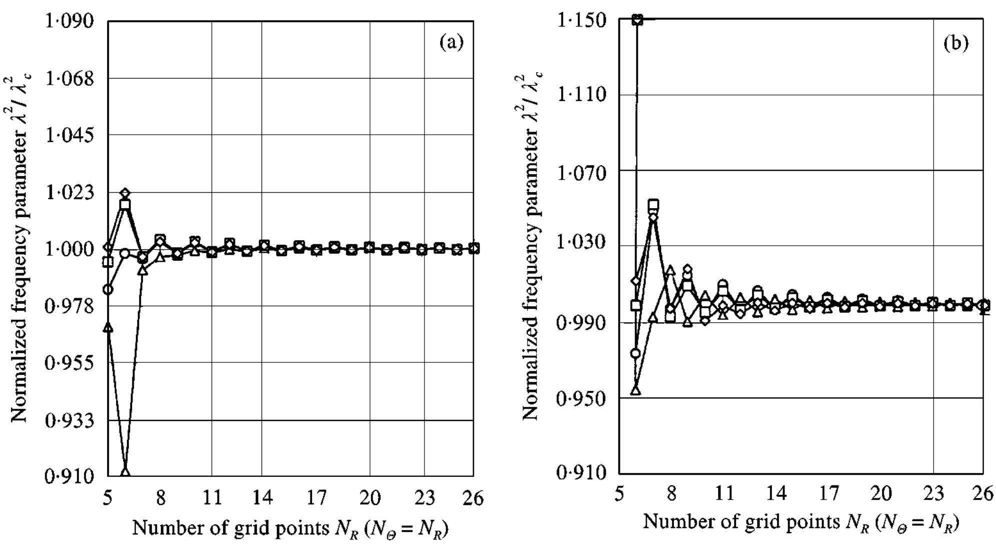

Figure 8. Effects of plate cut-out ratio b/a on convergence of normalized frequency parameter λ^2/λ_c^2 of annular sector plate with CFCF boundary conditions: (a) mode 1; (b) mode 5. —△—, $b/a = 0{\cdot}1$; —○—, $b/a = 0{\cdot}25$; —□—, $b/a = 0{\cdot}4$; —◇—, $b/a = 0{\cdot}5$.

inner-to-outer radius ratio b/a, but for the annular sector plate with CFCF boundary condition, the frequency parameters may increase for some modes such as the first and third modes in the case of $b/a = 0{\cdot}1$. This means that increasing the sector angles will lead to the decrease of the flexural stiffness for the annular sector plates with SSSS, CCCC, CSCS, FCSC and SCFC boundary conditions, but may not necessarily reduce the flexural stiffness for the CFCF plates.

TABLE 1

Comparison study of frequency parameters, $\lambda^2 = \omega a^2 \sqrt{\rho h/D}$, for annular sector plates with different boundary conditions

α (deg)	b/a	h/a	Boundary condition	Method used	Mode sequence 1	2	3	4	5
45	0·5	0·005	SSSS	DQM†	68·357	150·88	189·43	278·03	283·22
	0·5	Thin plate	SSSS	exact‡	68·380	150·96	189·61	278·46	283·59
30	0·5	0·1	SSSS	DQM†	88·486	171·23	199·86	275·09	280·69
	0·5	0·1	SSSS	FSM§	88·56	171·5	200·2	275·6	281·1
	0·5	0·1	SSSS	RRM¶	88·530	171·63	200·29	275·07	281·53
	0·5	0·2	SSSS	DQM†	67·237	115·82	131·55	170·76	173·78
	0·5	0·2	SSSS	FSM§	67·41	116·2	132·0	171·2	174·3
	0·5	0·2	SSSS	RRM¶	67·394	116·29	132·10	171·54	174·68
60	0·5	0·1	SSSS	DQM†	50·982	88·486	138·60	140·70	171·23
	0·5	0·1	SSSS	FSM§	51·02	88·56	138·9	140·9	171·5
	0·5	0·1	SSSS	RRM¶	51·025	88·530	138·94	140·89	171·63
	0·5	0·2	SSSS	DQM†	41·995	67·237	97·320	98·704	115·82
	0·5	0·2	SSSS	FSM§	42·07	67·41	97.62	99·00	116·2
	0·5	0·2	SSSS	RRM¶	42·066	67·394	97·698	99·040	116·29
90	0·00001	0·005	CCCC	DQM†	48·766	87·722	104·81	136·80	164·39
	0·00001	Thin plate	CCCC	exact‡	48·70	88·13	105·06	138·33	165·31
	0·5	0·005	CCCC	DQM†	95·140	114·83	150·35	201·07	252·73
	0·5	Thin plate	CCCC	exact‡	95·04	114·52	151·24	204·41	253·74
45	0·5	0·005	CSCS	DQM†	107·47	178·61	268·98	305·33	345·68
	0·5	Thin plate	CSCS	exact‡	107·63	178·77	169·13	309·34	353·27
60	0·5	0·1	CSCS	DQM†	76·902	103·68	150·41	167·33	191·59
	0·5	0·1	CSCS	FSM§	77·13	103·9	150·7	167·9	192·1
	0·5	0·1	CSCS	RRM¶	77·082	103·91	150·78	167·89	192·22
	0·5	0·2	CSCS	DQM†	53·099	72·152	101·11	103·02	119·41
	0·5	0·2	CSCS	FSM§	53·34	72·40	101·4	103·5	119·8
	0·5	0·2	CSCS	RRM¶	53·321	72·430	101·53	103·52	119·97
45	0·4	0·001	CFCF	DQM†	61·112	75·075	132·57	169·19	190·41
	0·4	0·001	CFCF	RRM¶	61·160	75·150	132·86	169·32	190·26
	0·4	0·2	CFCF	DQM†	37·292	42·403	71·603	77·536	85·595
	0·4	0·2	CFCF	RRM¶	37·441	42·552	71·804	77·890	85·947
90	0·4	0·1	CFCF	DQM†	51·304	53·649	63·660	84·339	114·59
	0·4	0·1	CFCF	RRM¶	51·406	53·760	63·785	84·497	114·82
	0·4	0·2	CFCF	DQM†	37·446	38·975	46·046	60·568	77·541
	0·4	0·2	CFCF	RRM¶	37·597	39·126	46·202	60·761	77·895

† Present differential quadrature method.
‡ Exact analytical method by Ramkrishnan and Kunukkasseril [2].
§ Finite-strip method by Mizusawa [15].
¶ Rayleigh–Ritz method by Xiang *et al.* [25].

TABLE 2

Frequency parameters, $\lambda^2 = \omega a^2 \sqrt{\rho h/D}$, for annular sector plates with SSSS boundary conditions

α (deg)	b/a	h/a	Mode of sequence 1	2	3	4	5	6
30	0·10	0·01	97·817	183·322	276·687	286·881	409·124	428·095
		0·10	84·440	143·881	199·711	205·375	268·226	277·275
		0·20	64·693	100·536	131·473	134·512	165·947	167·443
	0·25	0·01	97·828	183·597	276·686	289·176	418·904	428·089
		0·10	84·447	144·050	199·711	206·599	272·808	277·274
		0·20	64·697	100·628	131·473	135·143	167·286	169·732
	0·50	0·01	103·238	227·683	276·957	423·932	435·419	534·834
		0·10	88·486	171·234	199·860	275·089	280·693	325·311
		0·20	67·237	115·823	131·552	170·760	173·780	173·836
60	0·10	0·01	39·948	94·539	97·817	168·874	177·030	183·322
		0·10	37·366	81·937	84·440	134·424	139·820	143·881
		0·20	32·092	63·072	64·693	95·050	98·205	100·536
	0·25	0·01	40·835	97·828	101·379	177·030	183·597	191·747
		0·10	38·122	84·447	87·009	139·820	144·050	149·010
		0·20	32·633	64·697	66·211	98·205	100·628	103·261
	0·50	0·01	55·898	103·238	175·437	178·407	227·683	276·956
		0·10	50·982	88·486	138·598	140·702	171·234	199·860
		0·20	41·996	67·237	97·320	98·704	115·823	131·552
120	0·10	0·01	20·492	39·948	62·727	66·136	94·539	97·817
		0·10	19·675	37·366	56·463	59·535	81·937	84·440
		0·20	17·862	32·092	45·724	48·129	63·072	64·693
	0·25	0·01	24·076	40·835	66·248	78·861	97·827	101·379
		0·10	23·019	38·122	59·624	69·557	84·447	87·009
		0·20	20·612	32·633	48·186	54·668	64·697	66·211
	0·50	0·01	43·961	55·898	75·788	103·238	137·650	162·478
		0·10	40·778	50·982	67·272	88·486	113·335	130·056
		0·20	34·494	41·996	53·340	67·237	82·604	92·334

TABLE 3

Frequency parameters, $\lambda^2 = \omega a^2 \sqrt{\rho h/D}$, for annular sector plates with CCCC boundary conditions

α (deg)	b/a	h/a	Mode of sequence 1	2	3	4	5	6
30	0·10	0·01	187·056	297·335	412·551	424·333	569·715	590·374
		0·10	128·289	183·331	234·414	240·017	297·884	303·995
		0·20	81·177	110·699	136·614	141·531	171·828	173·966
	0·25	0·01	187·056	297·337	412·547	424·348	569·759	590·325
		0·10	128·290	183·366	234·414	240·451	300·161	303·995
		0·20	81·183	110·764	136·614	141·961	173·469	173·967
	0·50	0·01	190·942	338·662	412·663	562·649	595·274	714·458
		0·10	131·375	205·763	234·581	300·052	307·465	349·689
		0·20	83·457	123·157	136·780	173·724	176·299	198·360

TABLE 3 (*Continued*)

α (deg)	b/a	h/a	Mode of sequence 1	2	3	4	5	6
60	0·10	0·01	75·445	144·531	148·163	232·571	241·913	249·029
		0·10	62·412	108·355	110·727	159·482	164·547	167·779
		0·20	45·452	72·576	73·962	101·611	104·487	105·855
	0·25	0·01	75·874	148·165	149·750	241·864	249·154	253·613
		0·10	62·839	110·734	112·141	164·502	167·942	171·670
		0·20	45·853	73·975	74·973	104·342	106·017	108·612
	0·50	0·01	105·750	158·636	244·320	261·859	314·706	356·056
		0·10	82·164	116·624	165·724	169·620	198·127	221·583
		0·20	56·594	77·357	103·806	105·145	121·160	135·295
120	0·10	0·01	38·009	62·712	89·369	94·448	126·422	131·473
		0·10	34·218	53·974	73·698	77·387	99·601	102·533
		0·20	27·602	41·001	53·406	55·878	69·392	71·118
	0·25	0·01	45·421	64·539	94·114	116·003	130·199	139·097
		0·10	39·817	55·216	77·237	90·627	102·072	106·624
		0·20	31·056	41·814	55·951	62·420	71·127	72·862
	0·50	0·01	91·936	101·564	119·268	145·796	180·886	224·242
		0·10	72·317	79·149	91·761	109·959	132·549	158·272
		0·20	49·788	54·674	63·253	74·838	88·418	98·912

TABLE 4

Frequency parameters, $\lambda^2 = \omega a^2\sqrt{\rho h/D}$, for annular sector plates with CSCS boundary conditions

α (deg)	b/a	h/a	Mode of sequence 1	2	3	4	5	6
30	0·10	0·01	113·912	205·158	302·082	313·934	441·102	459·708
		0·10	93·450	152·635	206·900	213·083	274·652	283·188
		0·20	67·933	102·556	132·862	135·609	165·947	167·818
	0·25	0·01	114·047	206·885	302·081	322·509	459·708	466·302
		0·10	93·491	153·114	206·900	215·367	281·195	283·188
		0·20	67·946	102·712	132·862	136·414	167·286	170·310
	0·50	0·01	135·047	297·984	303·798	482·085	533·976	568·787
		0·10	103·682	191·593	207·276	288·449	293·159	330·323
		0·20	72·152	119·412	132·981	172·041	173·780	174·731
60	0·10	0·01	51·149	111·796	113·912	192·926	197·884	205·158
		0·10	45·840	91·764	93·450	144·269	148·134	152·635
		0·20	36·787	66·656	67·933	97·433	100·317	102·556
	0·25	0·01	55·913	114·047	130·885	197·886	206·885	238·049
		0·10	48·727	93·491	101·804	148·134	153·114	164·981
		0·20	38·137	67·946	71·004	100·317	102·712	106·541
	0·50	0·01	98·586	135·047	204·817	257·257	297·984	303·798
		0·10	76·902	103·682	150·413	167·327	191·593	207·276
		0·20	53·099	72·152	101·108	103·024	119·412	132·981

TABLE 4 (*Continued*)

α (deg)	b/a	h/a	Mode of sequence 1	2	3	4	5	6
120	0·10	0·01	31·730	51·149	79·752	83·049	111·796	113·912
		0·10	28·570	45·840	68·489	68·764	91·764	93·450
		0·20	23·678	36·787	50·975	52·087	66·656	67·933
	0·25	0·01	42·728	55·913	80·749	113·861	114·047	130·885
		0·10	37·415	48·727	68·915	89·097	93·491	101·804
		0·20	29·161	38·137	52·248	61·629	67·946	71·004
	0·50	0·01	91·198	98·586	112·749	135·047	165·879	204·813
		0·10	71·730	76·902	87·339	103·682	125·174	150·412
		0·20	49·296	53·099	60·813	72·152	85·948	98·802

TABLE 5

Frequency parameters, $\lambda^2 = \omega a^2\sqrt{\rho h/D}$, for annular sector plates with CFCF boundary conditions

α (deg)	b/a	h/a	Mode of sequence 1	2	3	4	5	6
30	0·10	0·01	25·208	57·687	71·714	134·539	142·769	214·384
		0·10	22·899	44·274	59·550	96·968	107·901	152·784
		0·20	18·907	30·786	43·501	62·626	73·053	93·078
	0·25	0·01	38·101	68·438	106·238	158·962	209·174	214·522
		0·10	33·525	53·091	83·363	113·967	146·217	155·742
		0·20	26·348	36·830	57·447	74·655	93·864	105·052
	0·50	0·01	87·768	113·532	225·328	241·877	280·166	414·370
		0·10	69·340	83·530	157·007	159·210	177·555	247·316
		0·20	47·924	55·145	96·171	105·689	109·390	150·750
60	0·10	0·01	25·948	37·927	73·138	87·650	94·937	144·922
		0·10	23·333	32·377	60·356	73·172	75·670	109·074
		0·20	19·111	25·558	43·790	54·719	54·829	73·532
	0·25	0·01	38·700	48·442	89·177	107·410	122·868	161·807
		0·10	34·045	41·016	73·542	84·271	94·253	123·847
		0·20	26·590	31·187	54·551	58·063	65·020	85·224
	0·50	0·01	88·299	95·342	122·393	176·818	242·992	252·931
		0·10	69·744	73·872	91·885	129·168	158·774	164·194
		0·20	48·080	50·551	62·967	87·122	96·732	100·911
120	0·10	0·01	26·607	29·742	43·782	68·445	74·154	80·196
		0·10	23·917	26·425	38·813	58·885	61·216	65·904
		0·20	19·426	21·569	31·362	44·309	45·102	48·653
	0·25	0·01	39·018	41·513	51·556	71·462	100·598	108·016
		0·10	34·381	36·177	44·214	60·501	82·771	84·842
		0·20	26·783	28·096	34·204	46·051	58·044	60·249
	0·50	0·01	88·596	90·300	96·821	109·012	128·056	155·011
		0·10	69·969	70·954	75·206	83·556	97·139	116·047
		0·20	48·176	48·823	51·613	57·522	67·088	79·603

TABLE 6

Frequency parameters, $\lambda^2 = \omega a^2\sqrt{\rho h/D}$, for annular sector plates with FCSC boundary conditions

			Mode of sequence					
α (deg)	b/a	h/a	1	2	3	4	5	6
30	0·10	0·01	164·744	270·541	381·218	392·709	532·584	553·774
		0·10	117·451	174·877	225·774	232·863	291·989	297·736
		0·20	76·120	108·731	134·641	140·259	171·529	172·924
	0·25	0·01	164·744	270·540	381·218	392·687	532·375	553·773
		0·10	117·433	174·827	225·699	232·598	290·929	297·689
		0·20	76·100	108·665	134·618	139·957	169·769	172·907
	0·50	0·01	164·287	260·459	365·713	381·206	549·096	552·856
		0·10	116·768	164·817	219·965	225·638	295·922	314·013
		0·20	75·306	100·278	134·507	135·602	170·904	178·246
60	0·10	0·01	61·366	125·725	129·094	208·799	218·162	224·722
		0·10	52·798	98·940	100·979	150·455	155·518	159·205
		0·20	40·140	69·360	70·050	99·310	101·624	103·774
	0·25	0·01	61·292	124·809	129·093	203·518	218·133	224·704
		0·10	52·640	97·856	100·975	143·874	155·501	159·129
		0·20	39·962	67·995	70·041	92·759	101·616	103·662
	0·50	0·01	56·957	112·173	127·479	209·481	217·704	237·054
		0·10	48·628	88·113	99·492	147·925	155·101	172·553
		0·20	36·269	63·523	68·671	96·583	101·211	114·661
120	0·10	0·01	27·473	50·182	71·384	79·186	108·689	113·945
		0·10	25·564	44·981	61·785	67·990	89·766	93·376
		0·20	21·803	36·076	47·523	51·656	65·775	67·618
	0·25	0·01	26·364	49·938	65·099	79·019	106·752	113·656
		0·10	24·526	44·696	55·230	67·841	87·993	93·192
		0·20	20·780	35·808	42·010	51·556	64·148	67·564
	0·50	0·01	21·433	45·088	74·395	76·806	103·058	110·811
		0·10	19·542	40·295	64·237	66·527	84·560	90·886
		0·20	16·408	32·224	48·889	52·411	62·893	65·870

TABLE 7

Frequency parameters, $\lambda^2 = \omega a^2\sqrt{\rho h/D}$, for annular sector plates with SCFC boundary conditions

			Mode of sequence					
α (deg)	b/a	h/a	1	2	3	4	5	6
30	0·10	0·01	100·946	193·907	264·113	302·423	428·251	437·366
		0·10	78·311	132·054	169·733	189·733	247·247	247·766
		0·20	53·930	83·343	103·580	116·436	145·414	146·051
	0·25	0·01	100·935	193·903	264·085	302·420	428·220	437·356
		0·10	78·311	132·054	169·733	189·689	247·248	247·586
		0·20	53·930	83·337	103·581	116·392	145·415	146·244

TABLE 7 (*Continued*)

α (deg)	b/a	h/a	Mode of sequence 1	2	3	4	5	6
	0·50	0·01	100·912	194·463	264·053	322·615	437·361	500·669
		0·10	78·280	132·778	169·733	208·024	247·349	275·278
		0·20	53·836	84·880	103·584	130·199	145·670	161·410
60	0·10	0·01	28·110	71·774	76·547	135·330	145·324	155·924
		0·10	25·767	60·447	63·647	104·588	111·480	116·889
		0·20	21·578	44·981	46·734	72·173	76·745	78·816
	0·25	0·01	28·104	71·765	76·446	135·314	145·857	155·919
		0·10	25·764	60·447	63·498	104·589	112·517	116·887
		0·20	21·566	44·981	46·695	72·176	78·487	78·825
	0·50	0·01	27·932	71·751	89·918	135·339	160·174	217·719
		0·10	25·524	60·431	75·236	104·587	120·507	154·325
		0·20	21·279	44·990	56·335	72·169	82·126	100·689
120	0·10	0·01	8·310	19·753	35·807	37·749	58·755	64·640
		0·10	8·084	18·636	32·722	34·351	51·686	56·149
		0·20	7·599	16·418	27·269	28·333	40·865	43·394
	0·25	0·01	8·209	19·743	36·490	39·091	58·760	64·862
		0·10	7·975	18·628	33·380	35·716	51·702	56·398
		0·20	7·484	16·412	27·889	29·703	40·878	43·776
	0·50	0·01	8·782	20·119	37·023	59·066	67·069	84·429
		0·10	8·502	18·945	33·761	51·926	59·717	72·510
		0·20	7·950	16·695	28·093	40·981	47·562	54·774

(2) As the relative thickness h/a increases, the frequency parameters for the annular sector plate with any boundary conditions will decrease greatly for any given sector angle, mode sequence and inner-to-outer radius ratio.

(3) For the CFCF annular sector plate, increasing the inner-to-outer radius ratio b/a from 0·1 to 0·5 will increase the values of frequency parameters regardless of the sector angle, mode sequences and relative thickness, but for other cases considered in this paper, the effect of inner-to-outer radius ratio b/a on the frequency parameter is not significant in the range of the values of b/a between 0·1 and 0·25; the effect will become significant in the range of the values of b/a from 0·25 to 0·5, and in this range, the frequency parameters for most vibration modes will increase whereas some modes of frequency parameters may decrease as the value of b/a increases.

For all the natural frequencies considered in these tables, except for the thin annular sector plate ($h/a = 0{\cdot}01$) with at least one free edge, using 17 grid points along each co-ordinate variable will achieve the completely converged DQ results with five significant digits. But for the thin annular sector plates ($h/a = 0{\cdot}01$) with at least one free edge such as CFCF, FCSC, or SCFC plates, using 17 grid points along each co-ordinate variable can only obtain the converged DQ results with three to four significant digits for some vibration modes. However, this has been accurate enough for the engineering applications.

5. CONCLUDING REMARKS

In this paper, the differential quadrature method has been applied to solve the free vibration problem of thick annular sector plates based on the Mindlin first order shear deformation theory. The first six natural frequencies have been calculated for the plates with arbitrary combinations of free, clamped and simply supported boundary conditions and with various relative thickness, sector angle and inner-to-outer radius ratios. The convergence characteristics of the DQ method have been carefully investigated for different boundary conditions, relative thicknesses, sector angles and inner-to-outer radius ratios. The numerical results show that the DQ method can yield accurate results for the title problem with a relatively small number of grid points.

REFERENCES

1. M. Ben-Amoz 1959 *Journal of Applied Mechanics* **26**, 136–137. Note on deflections and flexural vibrations of clamped sectorial plates.
2. R. Ramakrishnan and V. X. Kunukkasseril 1973 *Journal of Sound and Vibration* **30**, 127–129. Free vibration of annular sector plates.
3. H. Yonezawa 1962 *Proceedings of the American Society of Civil Engineers*, *Journal of Engineering Mechanics* **88**, 1–21. Moments and free vibrations in curved girder bridges.
4. I. E. Harik and H. R. Molaghasemi 1989 *Proceedings of the American Society of Civil Engineers*, *Journal of Engineering Mechanics* **115**, 2709–2722. Analytical solution to free vibration of sector plates.
5. I. E. Harik 1990 *Journal of Sound and Vibration* **138**, 542–528. Vibration of sector plates on elastic foundations.
6. K. Ramaiah and K. Vijayakumar 1974 *Journal of Sound and Vibration* **34**, 53–61. Natural frequencies of circumferentially truncated sector plates with simply supported straight edges.
7. M. Mukhopadhyay 1982 *Journal of Sound and Vibration* **80**, 275–279. Free vibration of annular sector plates with edges possessing different degrees of rotational restraint.
8. T. Irie, K. Tanaka and G. Yamada 1988 *Journal of Sound and Vibration* **122**, 69–78. Free vibration of a cantilever annular sector plate with curved radial edges.
9. C. S. Kim and S. M. Dickinson 1989 *Journal of Sound and Vibration* **134**, 407–421. On the free vibration of annular and circular, thin, sectorial plates subject to certain complicating effects.
10. T. Irie G. Yamada, and F. Ito 1979 *Journal of Sound and Vibration* **67**, 89–100. Free vibration of polar orthotropic sector plates.
11. K. M. Liew and K. Y. Lam 1993 *International Journal of Mechanical Sciences* **35**, 129–139. On the use of 2-D orthogonal polynomials in the Rayleigh–Ritz method for flexural vibration of annular sector plates of arbitrary shape.
12. R. S. Srinivasan and V. Thiruvenkatachari 1983 *Journal of Sound and Vibration* **80**, 275–279. Free vibration of annular sector plates by an integral equation technique.
13. Y. K. Cheung and M. S. Cheung 1971 *Proceedings of the American Society of Civil Engineers*, *Journal of Engineering Mechanics* **97**, 391–441. Flexural vibrations of rectangular and other polygonal plates.
14. T. Mizusawa 1991 *Journal of Sound and Vibration* **149**, 461–470. Application of the spline element method to analyze vibration of annular sector plates.
15. T. Mizusawa 1991 *Journal of Sound and Vibration* **150**, 245–259. Vibration of thick annular sector plates using semi-analytical methods.
16. A. P. Bhattacharya and K. K. Bhowmic 1975 *Journal of Sound and Vibration* **41**, 503–505. Free vibration of a sector plate.

17. H. Kobayashi, T. Nishikawa and K. Sonoda 1987 *Proceedings of International Symposium on Geomechanics, Bridges and Structures, Lanzhou China*, 171–185. Effect of shear deformation on dynamic response of curved bridge to moving loads.
18. C. S. Huang, O. G. Mcgee and A. W. Leissa 1994 *International Journal of Solids and Structures* **31**, 1609–1631. Exact analytical solutions for free vibration of thick sectorial plates with simply supported radial edges.
19. K. Tanaka, G. Yamada, Y. Kobayashi and S. Miura 1990 *Journal of Sound and Vibration* **143**, 329–341. Free vibration of a cantilever annular sector plate with curved radial edges and varying thickness.
20. M. N. Bapu Rao, P. Guruswamy and K. S. Sampath Kumaran 1977 *Nuclear Engineering and Design* **41**, 247–255. Finite element analysis of thick annular and sector plates.
21. P. Guruswamy and T. Y. Yang 1979 *Journal of Sound and Vibration* **62**, 505–516. A sector element for dynamic analysis of thick plates.
22. R. S. Srinivasan and V. Thiruvenkatachari 1985 *Journal of Sound and Vibration* **101**, 193–210. Free vibration of transverse isotropic annular sector Mindlin plates.
23. P. R. Benson and E. Hinton 1976 *International Journal for Numerical Methods in Engineering* **10**, 665–678. A thick finite strip solution for static, free vibration and stability problems.
24. M. S. Cheung and M. Y. T. Chan 1981 *Computers and Structures* **14**, 79–88. Static and dynamic analysis of thin and thick sectorial plates by the finite strip method.
25. Y. Xiang, K. M. Liew and S. Kitipornchai 1993 *Proceedings of the American Society of Civil Engineers, Journal of Engineering Mechanics* **119**, 1579–1599. Transverse vibration of thick annular sector plates.
26. R. E. Bellman and J. Casti 1971 *Journal of Mathematical Analysis and Applications* **34**, 235–238. Differential quadrature and long term integration.
27. R. E. Bellman, B. G. Kashef and J. Casti 1972 *Journal of Computational Physics* **10**, 40–52. Differential quadrature: a technique for the rapid solution of nonlinear partial differential equations.
28. J. R. Quan and C. T. Chang 1989 *Computers in Chemical Engineering* **13**, 779–788. New insights in solving distributed system equations by the quadrature method—I. Analysis.
29. C. Shu and B. E. Richards 1992 *Journal of Numerical Methods in Fluids* **15**, 791–798. Application of generalized differential quadrature to solve two-dimensional incompressible Navier–Stokes equations.
30. C. W. Bert, S. K. Jang and A. G. Striz 1988 *AIAA Journal* **26**, 612–618. Two new approximate methods for analyzing free vibration of structural components.
31. C. W. Bert, S. K. Jang and A. G. Striz 1989 *Computational Mechanics* **5**, 217–226. Nonlinear bending analysis of orthotropic rectangular plates by the method of differential quadrature.
32. A. R. Kukreti, J. Farsa and C. W. Bert 1992 *Proceedings of the American Society of Civil Engineers, Journal of Engineering Mechanics* **118**, 1221–1237. Fundamental frequency of tapered plates by differential quadrature.
33. A. G. Striz, S. K. Jang and C. W. Bert 1988 *Thin-Walled Structures* **69**, 51–62. Nonlinear bending analysis of thin circular plates by differential quadrature.
34. R. D. Mindlin and H. Deresiewicz 1954 *Journal of Applied Physics* **25**, 1329–1332. Thickness-shear and flexural vibrations of a circular disk.
35. C. W. Bert and M. Malik 1996 *International Journal of Mechanical Sciences* **38**, 589–606. The differential quadrature method for irregular domains and application to plate vibration.
36. M. Malik and C. W. Bert 1997 *Applied Mechanics in the Americas* (*PACAM V*, *San Juan Puerto Rico*) **5**, 228–231. Differential quadrature analysis for curvilinear domains via geometric mapping by blending functions.